JOURNAL OF MATERIALS SCIENCE 21 (1986) 649–658

Synthesis and structure of chemically vapour-deposited boron nitride

TOSHITSUGU MATSUDA, NAOKI UNO, HIROYUKI NAKAE
Special Ceramics Group, Masumoto Amorphous and Intercalation Compounds Project, Research Development Corporation of Japan, 9-15, Futaba 2-chome, Shinagawa-ku, Tokyo 142, Japan

TOSHIO HIRAI
The Research Institute for Iron, Steel and Other Metals, Tohoku University, Sendai 980, Japan

Chemically vapour-deposited boron nitride (CVD-BN) plates have been synthesized on a graphite substrate by the reaction of the BCl_3–NH_3–H_2 gas system in a deposition temperature (T_{dep}) range from 1200 to 2000° C, with a total gas pressure (P_{tot}) which was varied from 5 to 60 torr. The effects of P_{tot} and T_{dep} on the crystal structure and the microstructure of the CVD-BN plate were investigated. Turbostratic BN(t-BN) was deposited above 10 torr, at any T_{dep} in the range investigated. The interlayer spacing ($c_0/2$), the crystallite size (Lc) and the preferred orientation (PO) were strongly affected by T_{dep}. The t-BN obtained at low T_{dep} had large $c_0/2$ and small Lc and PO. As T_{dep} increased, $c_0/2$ tended to decrease whereas Lc increased and the c-plane of the crystallites became oriented parallel to the deposition surface. At a P_{tot} of 5 torr, a mixture of t-BN and h-BN (hexagonal BN) was deposited at any T_{dep} above 1700° C, and two kinds of t-BN different in $c_0/2$ co-deposited at a T_{dep} below 1600° C. Moreover, it was indicated that r-BN (rhombohedral BN) was included in the deposits obtained at a P_{tot} of 5 torr and a T_{dep} of 1500 to 1600° C.

1. Introduction

In general, a boron nitride (BN) body is manufactured by the sintering of hexagonal BN powder with added sintering agents such as boric oxide, borate and high silicate glass, since BN alone is difficult to sinter [1, 2]. Therefore, unfavourable pores and impurities are apt to be included in the sintered body. On the other hand, the chemical vapour deposition (CVD) method enables the formation of high purity BN bodies with high density. Although various reaction gas systems have been reported for the syntheses of CVD-BN, the B_2H_6–NH_3 and BCl_3–NH_3 systems are generally used for the manufacture of films and free-standing bodies. The importance of free-standing bodies made from CVD-BN has been increasing, since they are frequently used in crucibles for melting semiconductor materials, and for high-temperature jigs and insulators. Basche and Shiff [3] reported on the properties of CVD-BN synthesized at a deposition temperature (T_{dep}) of 1900° C using the BCl_3–NH_3 system, and indicated that the material was useful in industrial applications. Similarly, Clerc and Gerlach [4] synthesized CVD-BN using the BCl_3–NH_3 system at a T_{dep} of 1500 to 1900° C and studied the high-temperature compatibility with various metals. Malé and Salanoubat [5] investigated the influence of H_2 on CVD in the BCl_3–NH_3 system. In these previous works, however, the effects of the formation conditions on the crystal structure, density and microstructure of CVD-BN, and its formation mechanism have not been reported on in any great detail. The present report describes the synthesis of CVD-BN plates of 0.2 to 1 mm in thickness, and the effects of the formation conditions on the crystal structure and microstructure.

2. Experimental procedure

2.1. Synthesis of CVD-BN plate

Fig. 1 is a schematic drawing of the CVD apparatus (Tachibana Riko CVD-250-T4). The 40 mm × 13 mm × 2 mm graphite substrate finished with No. 1500 emery paper was heated directly by electric current. Deposition temperature (T_{dep}) was measured with a two-colour pyrometer (Chino IR-Q2C) and was controlled automatically. T_{dep} was varied in the range from 1200 to 2000° C. BCl_3 (purity: 99.9%) and NH_3 (99.95%) gases were used for the starting materials and H_2 (99.999%) for dilution. Since BCl_3 readily reacts with NH_3 at room temperature and forms a white powder, these gases were introduced separately into the CVD reactor through a coaxial double tube in order to mix them in the vicinity of the substrate. NH_3 gas and a gas mixture of BCl_3 and H_2 were introduced through the inner and outer tubes, respectively. The gas-flow rates were kept constant at 90 standard cubic centimetre per minute (SCCM) for NH_3, 140 SCCM for BCl_3, and 670 SCCM for H_2. The total gas pressure (P_{tot}) in the CVD reactor was measured with a mercury manometer and was kept constant at a programmed pressure with a pressure

0022–2461/86 $03.00 + .12

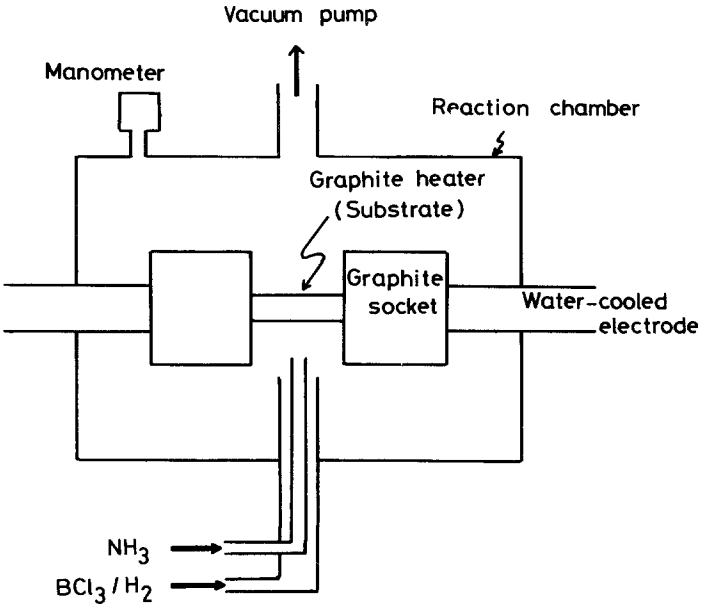

Figure 1 Reactor for the CVD-BN plate synthesis.

control valve attached to the exhaust side. The P_{tot} was varied in the range of 5 to 60 torr (0.67 to 8 kPa).

The deposit (CVD-BN plate) was completely removed from the graphite substrate using a diamond cutter and emery paper. The CVD-BN plate obtained was about 30 mm × 11 mm × 0.2 to 1 mm in size and subjected to the measurements described below.

2.2. Crystal structure analysis

The plate sample was reduced to powder by vibratory milling in an alumina mill. The powdered sample (−325 mesh) was subjected to X-ray diffraction to obtain interlayer spacing ($c_0/2$), the apparent crystallite size of the c-axis direction (Lc), and the preferred orientation of the crystallites (PO), using an X-ray diffractometer with Ni-filtered Cu$K\alpha$-radiation (Rigaku Geigerflex 2013). $c_0/2$ was calculated using the half-width mid-points of the (0 0 2) and (0 0 4) reflections. The Lc was calculated using the Scherrer equation ($Lc = K\lambda/B\cos\theta$) substituting the half width of the (0 0 2) reflection, where K was taken as 0.9 [6]. The integrated intensities for the (0 0 2) and (1 0) reflections [I(0 0 2) and I(1 0)] were measured to estimate PO according to the following equation:

$$PO = \frac{[I(1\,0)/I(0\,0\,2)]_{plate}}{[I(1\,0)/I(0\,0\,2)]_{powder}} \quad (1)$$

The numerator and the denominator of the above equation respectively represent the integrated ratio of the (1 0) to (0 0 2) reflection for the powdered and plate samples.

2.3. Microstructure observation

The deposition surface and the fracture surface vertical to the deposition surface of the CVD-BN plate were observed with a scanning electron microscope (SEM) (Hitachi H-800). The sample surface was ultrasonically cleaned in acetone and was coated with a gold film having a thickness of about 30 nm.

3. Results

The appearance of the CVD-BN plate varied from colourless transparent to white opaque, depending on the deposition conditions. Transparent plates were obtained at a T_{dep} below 1400° C and a P_{tot} above 20 torr. The plates tended to turn opaque as T_{dep} and P_{tot} were increased and decreased, respectively. Fig. 2 shows (a) a 0.7 mm-thick transparent plate and (b) a 0.5 mm-thick white opaque plate. Transparent plates gradually became cloudy with exposure to the atmosphere, which finally produced cracks in some of the plates. The plates generated an NH_3 odour when they were being reduced to powder. They also gained weight in the atmosphere. These results indicated that the transparent plates showed instability when exposed to moisture. These phenomena observed on the transparent plates were not seen in the white opaque plates.

CVD-BN plates with uniform thickness were obtained on the substrate at a low P_{tot}, while thickness tended to become non-uniform as P_{tot} increased. For the CVD-BN plate obtained at a P_{tot} of 60 torr and a T_{dep} of 1600° C, for example, the thickness at the end part of the substrate under the upper stream of the source gases was several times thicker than that at the

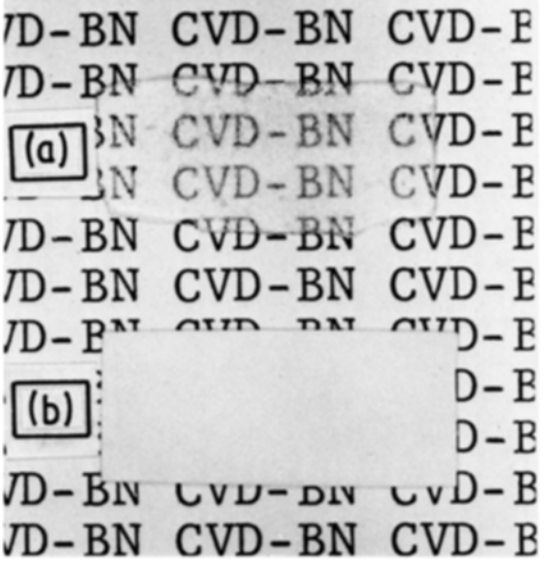

Figure 2 Transparent and white opaque CVD-BN plates. (a) T_{dep} = 1400° C, P_{tot} = 30 torr (thickness = 0.7 mm); (b) T_{dep} = 1800° C, P_{tot} = 5 torr (thickness = 0.5 mm).

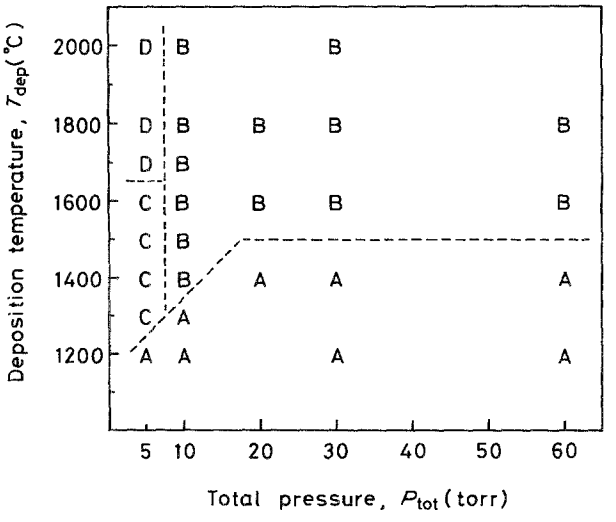

Figure 3 Effects of T_{dep} and P_{tot} on the crystal structure of the CVD-BN plates. Type A, isotropic t-BN; Type B, anisotropic t-BN; Type C, (t + t')-BN; Type D, (t + h)-BN.

centre part of the substrate. In the CVD-BN plates with a non-uniform thickness, only the centre part of the plate was subjected to various measurements.

3.1. Crystal structure of CVD-BN

The CVD-BN plates obtained were classified into four types (A to D) according to their transparency and crystal structure. The formation of these four types of deposits depended on T_{dep} and P_{tot}, as shown in Fig. 3.

The deposits obtained at a P_{tot} of 10 to 60 torr yielded the X-ray diffraction patterns given in Fig. 4a and b. The fact that no (1 0 1) reflection is observed in the (1 0) band means a structure lacking three-dimensional ordering, which could be identified as the so-called turbostratic BN(t-BN) [6]. t-BN, which is characterized by broad (0 0 l) reflections as shown in Fig. 4a, was obtained at a low T_{dep} (in the region marked with A in Fig. 3). This t-BN plate showed high transparency. The transparency was reduced as T_{dep} increased, so that the appearance of the CVD-BN plates obtained in the B-region in Fig. 3 varied from semi-transparent to white opaque. Sharper (0 0 l) reflections were obtained for those deposits, as can be seen in Fig. 4b. As will be described later, the continuous change in $c_0/2$ of the t-BN deposited in the A- and B-regions suggests similarity in crystal structure. However, the A-region deposits showed a different orientation and fracture behaviour from the B-region deposits; i.e. the CVD-BN plates in the A-region were isotropic, and CVD-BN plates in the B-region were anisotropic. Accordingly, the region of the t-BN formation was classified into two (A and B) regions for convenience.

Fig. 4c is an example of the X-ray diffraction pattern for the deposit formed in the C-region (P_{tot} of 5 torr and T_{dep} of 1300 to 1600° C). Two (0 0 2) and two (0 0 4) reflections indicate that the deposit was composed of two kinds of BN having different $c_0/2$. The (0 0 l) reflections at the low angles [$(0\,0\,l)_L$] were near to those of t-BN formed at a P_{tot} of 10 torr and at the same T_{dep}, while the (0 0 l) reflections at high angles

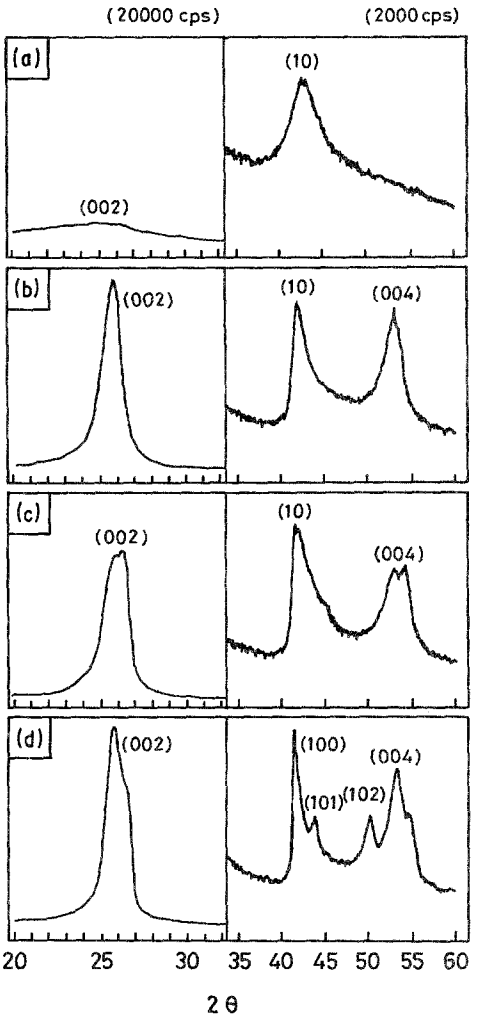

Figure 4 Typical X-ray diffraction pattern of powdered CVD-BN. (a) Type A, isotropic t-BN (T_{dep} = 1200° C, P_{tot} = 30 torr); (b) Type B, anisotropic t-BN (T_{dep} = 1600° C, P_{tot} = 30 torr); (c) Type C, (t + t')-BN (T_{dep} = 1600° C, P_{tot} = 5 torr); (d) Type D, (t + h)-BN (T_{dep} = 2000° C, P_{tot} = 5 torr), (Cu$K\alpha$ radiation filtered with Ni).

[$(0\,0\,l)_H$] were attributed to the BN with smaller $c_0/2$ newly formed in the C-region. The $c_0/2$ of the latter BN with the $(0\,0\,l)_H$ reflections was very close to that of h-BN [7]; however, no (1 0 1) or (1 0 2) reflections indicating three-dimensional ordering were seen in the (1 0) band. This observation suggests that the BN which yields the $(0\,0\,l)_H$ reflections also has a disordered structure. This turbostratic BN with a smaller $c_0/2$ was denoted as t'-BN in order to distinguish it from the t-BN yielding the $(0\,0\,l)_L$ reflections. Accordingly, the C-region deposits were denoted as (t + t')-BN. A slight shoulder was recognized at 2θ of 45.5° in the (1 0) band of the deposits obtained at a T_{dep} of 1600 (Fig. 4c) and 1500° C, as discussed later. The CVD-BN plates obtained in the C-region ranged from semi-transparent to white opaque.

Fig. 4d is an example of the X-ray diffraction pattern of the deposit formed in the D-region (P_{tot} of 5 torr and T_{dep} above 1700° C). As in the C-region deposits, the (0 0 2) and (0 0 4) reflections yielded two peaks each; therefore, the deposit was identified as a mixture of two kinds of BN having different $c_0/2$. In Fig. 4d, however, the (1 0 1) and (1 0 2) reflections were clearly recognized, indicating the presence of h-BN with three-dimensional ordering. The diffraction angles for $(0\,0\,l)_L$

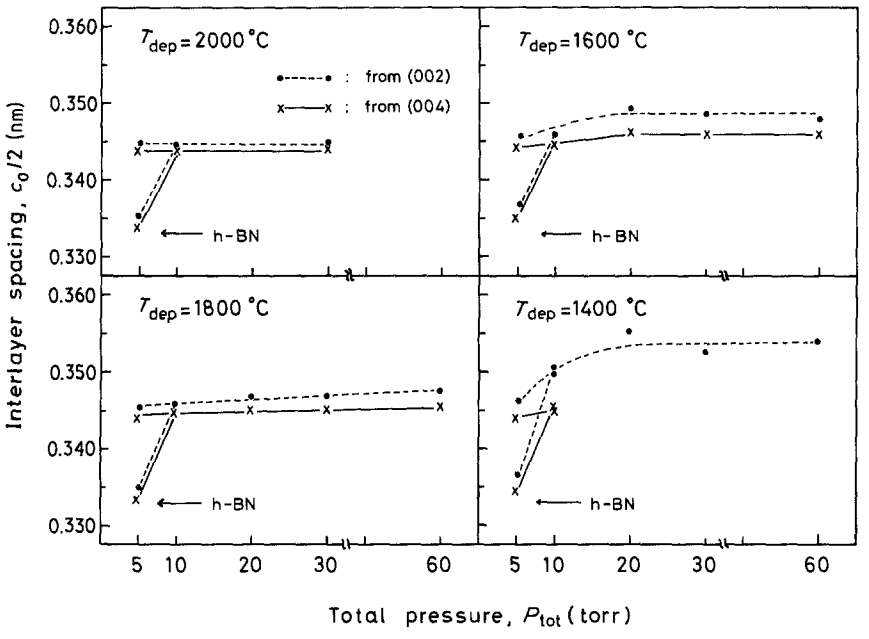

Figure 5 Effect of P_{tot} on the interlayer spacing, (●——●) $c_{0(002)}/2$ from (0 0 2) and (×——×) $c_{0(004)}/2$ from (0 0 4).

reflections corresponded to those of t-BN that were formed in the B-region. The deposits obtained in the D-region are therefore denoted as (t + h)-BN. These CVD-BN plates were white opaque in appearance.

In Fig. 5 the change of $c_0/2$ against P_{tot} is plotted. The solid lines and dotted lines represent $c_0/2$ values obtained from the (0 0 4) and (0 0 2) reflections, respectively. In the case of the deposits formed at a P_{tot} of 5 torr, the double peaks of the (0 0 l) reflections shown in Fig. 4c and d were separated using a computer for calculating precise $c_0/2$ values. P_{tot} only slightly affected $c_0/2$ at a P_{tot} of 10 to 60 torr. At a P_{tot} of 5 torr, h-BN with $c_{0(004)}/2$ of 0.333 nm was obtained, mixed with t-BN with $c_{0(004)}/2$ of 0.344 nm at a T_{dep} of 1700 to 2000° C, whereas t'-BN with $c_{0(004)}/2$ near to that of h-BN was co-deposited with t-BN at a T_{dep} of 1300 to 1600° C. Fig. 6 shows the change of $c_{0(002)}/2$ with T_{dep}. As shown in Fig. 6, BN with a smaller $c_0/2$ is formed at high temperatures, except for a P_{tot} of 5 torr.

The relation between the apparent crystallite size in the c-direction (Lc) and the deposition condition is shown in Fig. 7. Lc for deposits formed at a P_{tot} above 10 torr are given in this figure. Lc was larger for the higher T_{dep} and for the lower P_{tot}. Lc for the deposits formed at a P_{tot} of 5 torr was not obtained with any degree of accuracy due to the double peaks; however, Lc for t-BN, having the $(0\,0\,l)_L$ reflections, formed at a T_{dep} above 1700° C was similar to that for the deposit obtained at a P_{tot} of 10 torr. Lc of h-BN with the $(0\,0\,l)_H$ reflections was estimated from the separated peak to be in the range from several tens to a hundred nanometers.

Fig. 8 gives the relation between the relative intensity ratio $I(1\,0)/I(0\,0\,2)$ of a plate sample to that of a powdered sample and the deposition conditions. At a P_{tot} above 10 torr, the c-plane of BN tended to be more parallel to the deposition surface as T_{dep} increased. Relatively isotropic CVD-BN plates were obtained at a T_{dep} below 1400° C (A-region in Fig. 3). On the other hand, at a P_{tot} of 5 torr, preferred orientations were observed at any T_{dep}, and were especially prominent at T_{dep} of 1400 and 1300° C.

3.2. Microstructure of the deposition surface and fracture surface of the CVD-BN plate

A pebble-like structure was observed by SEM at low magnification on all the deposition surfaces. Fig. 9a

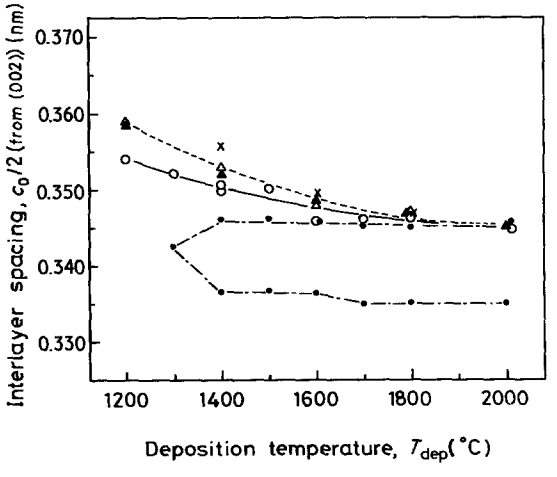

Figure 6 Effect of T_{dep} on the interlayer spacing, $c_{0(002)}/2$. P_{tot}(torr); (●) 5, (○) 10, (×) 20, (▲) 30 and (△) 60.

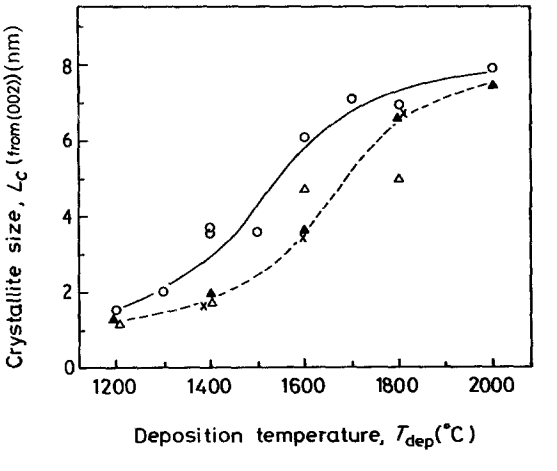

Figure 7 Effect of T_{dep} on the apparent crystallite size, Lc. P_{tot}(torr); (○) 10, (×) 20, (▲) 30 and (△) 60.

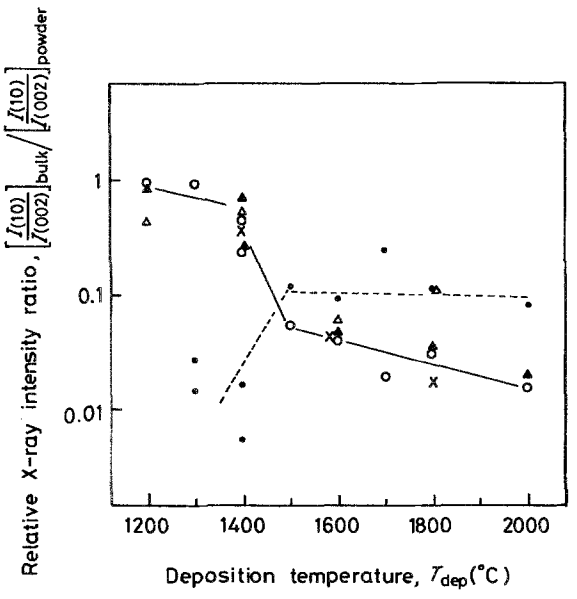

Figure 8 Effect of T_{dep} on the preferred orientation of the CVD-BN plates. P_{tot}(torr); (●) 5, (○) 10, (×) 20, (▲) 30 and (△) 60.

and b are SEM photographs (× 50) of the t-BN plates obtained in the A-region and the (t + h)-BN plates obtained in the D-region, respectively. The pebble sizes tended to be larger for lower T_{dep} and higher P_{tot}. SEM observation at high magnification (× 20 000) clarified that these pebbles were composed of fine grains. Figs. 10a to d are high magnification SEM photographs of the deposition surfaces of the CVD-BN plates obtained in the regions from A to D in Fig. 3. Finer grains of less than 0.1 μm in diameter were observed in the regions from A to C, independent of T_{dep} and P_{tot}, whereas in the D-region, grains more than ten times larger were observed.

Figs. 11a to d are SEM photographs of the fracture surfaces of the CVD-BN plates obtained in the regions from A to D. All CVD-BN plates obtained in the A-region exhibited glass-like fracture surfaces as shown in Fig. 11a. In contrast, Figs. 11b to d show the laminar fracture surface for the CVD-BN plates obtained in the regions from B to D.

4. Discussion

4.1. Synthesis of CVD-BN plate

Syntheses of CVD-BN have been examined using such boron compounds as B_2H_6 [8–15], BCl_3 [3–5, 16–24], BF_3 [25–28], $B_3N_3H_6$ [29], $B_3N_3H_3Cl_3$ [30], $B_{10}H_{14}$ [31], $(C_2H_5)_3B$ [32], etc. Most of the previous research has been concentrated on syntheses using BCl_3 or B_2H_6, since these two are sufficiently high in vapour pressure at room temperature. BCl_3 is easier to handle than B_2H_6. In addition, the high thermal stability of BCl_3 [33] enables synthesis at a higher T_{dep}. In the region where the surface reaction is the rate limiting step in the CVD process, the deposition rate is larger for higher T_{dep}. Therefore, the BCl_3–NH_3 system is better for obtaining a thick plate or free-standing body of CVD-BN.

Meyer and Zappner [34] and Tagawa and Ishii [35] reported that BCl_3 and NH_3 readily react with each other at room temperature to form white powder with the chemical composition of B : N : Cl = 1 : 4 : 3 (atomic ratio). The powder is probably composed of boron amide compounds, boron imide compounds and ammonium chloride. Thus, the mixing zone of BCl_3 and NH_3 gases is one of the important factors for the synthesis of CVD-BN bodies using the BCl_3–NH_3 system. Basche [17] mixed the source gases in a temperature range from 150 to 200° C and filtered off the by-product powder to synthesize CVD-BN, whereas other researchers [4, 5, 18, 20–22] adopted various other methods of introducing BCl_3 and NH_3 separately into the reactor. Clerc and Gerlach [4] mixed BCl_3 and NH_3 at a distance of 90 mm from the substrate. Takahashi *et al.* [20–22] mixed the gases at 50 and 20 mm. The present authors carried out preliminary experiments on the mixing zone of BCl_3 and NH_3, using a coaxial double tube to determine the optimum distance between the substrate and the end of the tube. It was found that at longer distances more by-products, mainly consisting of NH_4Cl, grew at the end of the tube and that the deposition rate decreased. Considering these results, a distance of 20 mm was chosen for the present experiments. Niihara and Hirai [36] succeeded in the synthesis of a Si_3N_4 plate at high deposition

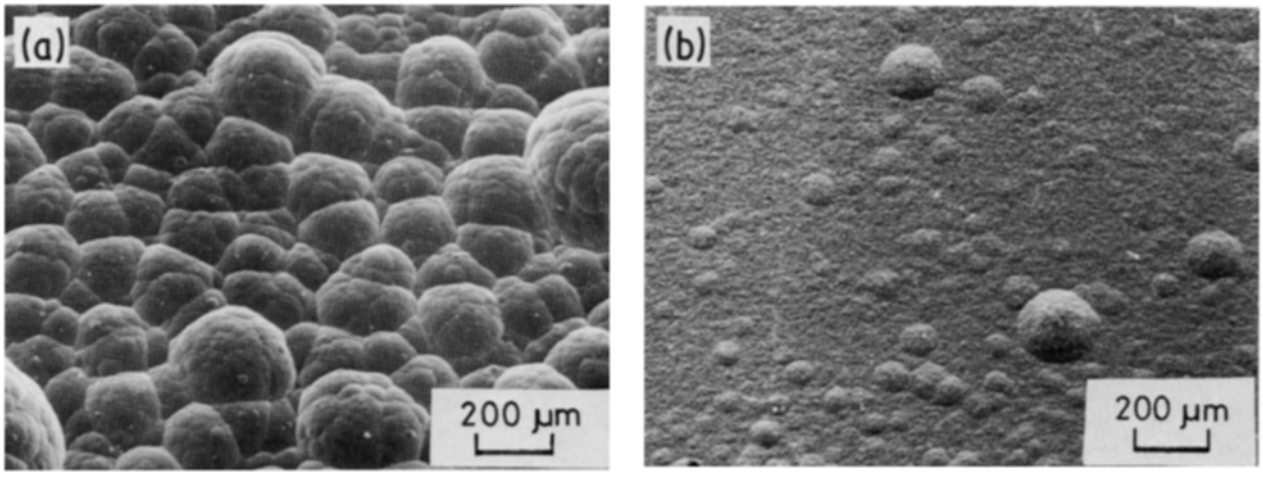

Figure 9 SEM-photographs of deposition surface of the CVD-BN plates. (a) The t-BN plate prepared at T_{dep} = 1400° C, P_{tot} = 30 torr in the A-region; (b) the (t + h)-BN plate prepared at T_{dep} = 2000° C, P_{tot} = 5 torr in the D-region.

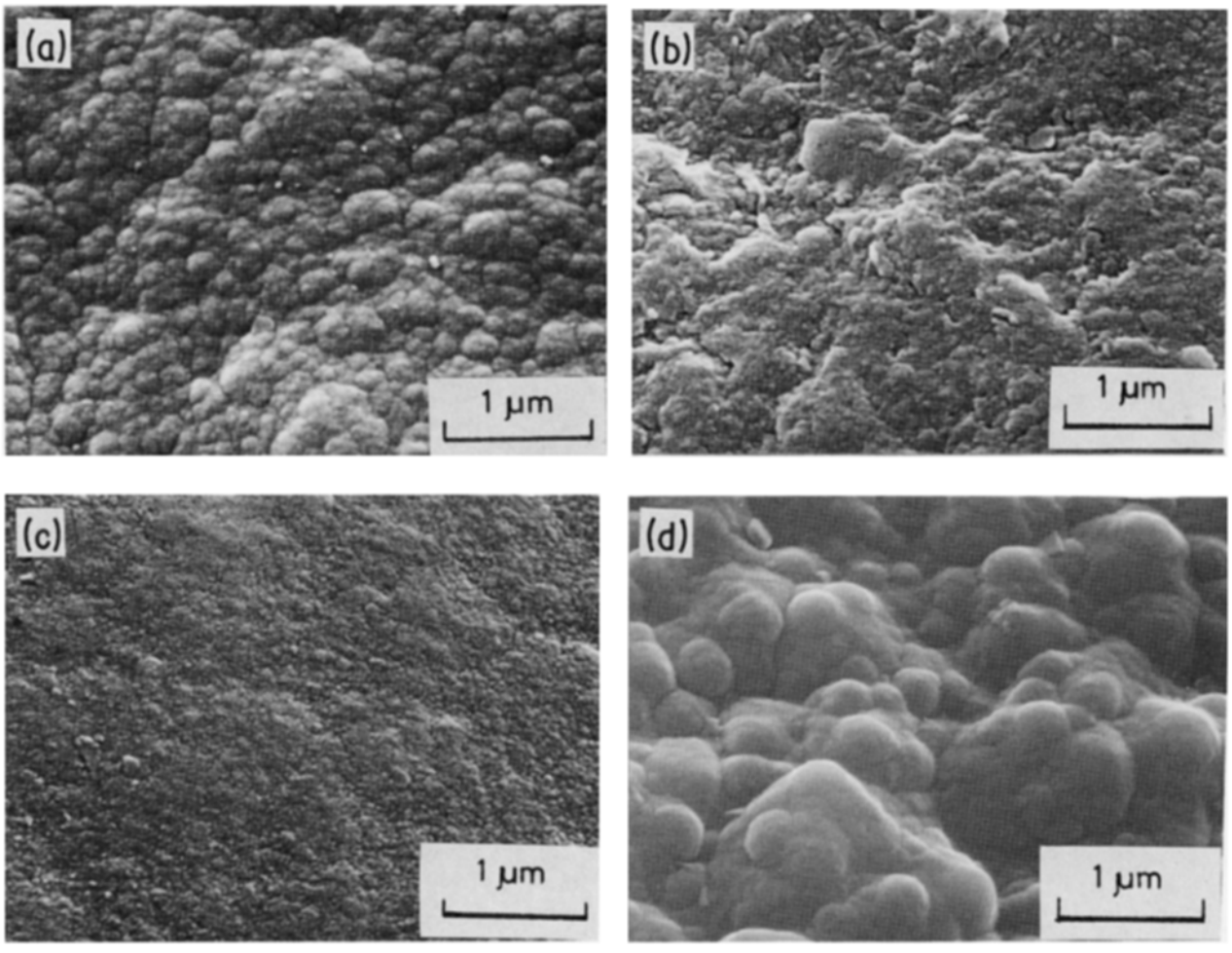

Figure 10 SEM-photographs at a high magnification of the deposition surface of the CVD-BN plates. (a) The t-BN plate prepared at a T_{dep} = 1400° C, P_{tot} = 30 torr in the A-region; (b) the t-BN plate prepared at a T_{dep} = 2000° C, P_{tot} = 30 torr in the B-region: (c) the (t + t′)-BN plate prepared at a T_{dep} = 1400° C, P_{tot} = 5 torr in the C-region; (d) the (t + h)-BN plate prepared at a T_{dep} = 2000° C, P_{tot} = 5 torr in the D-region.

rates by mixing $SiCl_4$ and NH_3 at a position 20 mm away from the substrate. For the BCl_3–NH_3 and $SiCl_4$–NH_3 systems, since intermediates are readily formed, structures of the intermediates may vary according to the mixing methods. The variation in structure of the intermediates seems to affect the crystallinity of the deposits and the deposition rate. For the BCl_3–NH_3 system, Clerc and Gerlach [4] reported that the deposit was powder at a P_{tot} above 2 torr. Moreover, Malé and Salanoubat [5], and Basche and Shiff [3] showed that the optimum P_{tot} for the preparation of a CVD-BN body was 1 to 2 torr. In the present experiments, however, CVD-BN plates with good crystallinity were successfully obtained at a P_{tot} of 5 torr by adopting our original mixing method.

4.2. Crystal structure of CVD-BN plate

BN has five different structures: h-BN (hexagonal), r-BN (rhombohedral) and a-BN (amorphous, including turbostratic structure t-BN) at ordinary pressure; w-BN (wurtzite-type) and c- or z-BN (cubic or zincblende-type) at high pressure. It has recently been reported that a high pressure phase BN (thin film) was obtained from the vapour phase using plasma or ion-beam techniques [37–39]; however, the common thermal CVD method only yields ordinary pressure phases (Table I). Many researchers report that CVD-BN is t-BN with a $c_0/2$ larger than that of h-BN. No systematic studies on the effect of the deposition condition regarding $c_0/2$ and Lc of CVD-BN have yet been made. The reported values of $c_0/2$ and Lc are listed in Table I. The term "turbostratic structure (t-)" is applied to the three-dimensionally disordered structure with two-dimensional ordering [40]. t-BN is characterized by an X-ray diffraction pattern yielding no ($h\,k\,l$) reflections. Takahashi *et al.* [20–22] reported that the CVD-BN formed on iron and nickel substrates were well-crystallized BN with $c_0/2$ of 0.333 nm; however, no reference was made to the ($h\,k\,l$) reflections which are indicative of three-dimensional ordering.

In the present experiments, a t-BN plate was obtained in all cases at a P_{tot} above 10 torr. The $c_0/2$ of t-BN decreased and Lc increased as T_{dep} increased. Nakamura and Arai [41] obtained t-BN powder by heat-treating the intermediates obtained by the reaction of BCl_3 and NH_3 gases at room temperature. The reported values of $c_0/2$ and Lc for the t-BN are as follows: $c_0/2$ = 0.36 nm and Lc = 1.5 nm for heat treatment at 1200° C for 2 h; $c_0/2$ = 0.34 nm and Lc = 10.0 nm at 2000° C for 2 h. Both values are in good agreement with the T_{dep} dependence of $c_0/2$ and Lc of the present t-BN obtained at a P_{tot} above 10 torr.

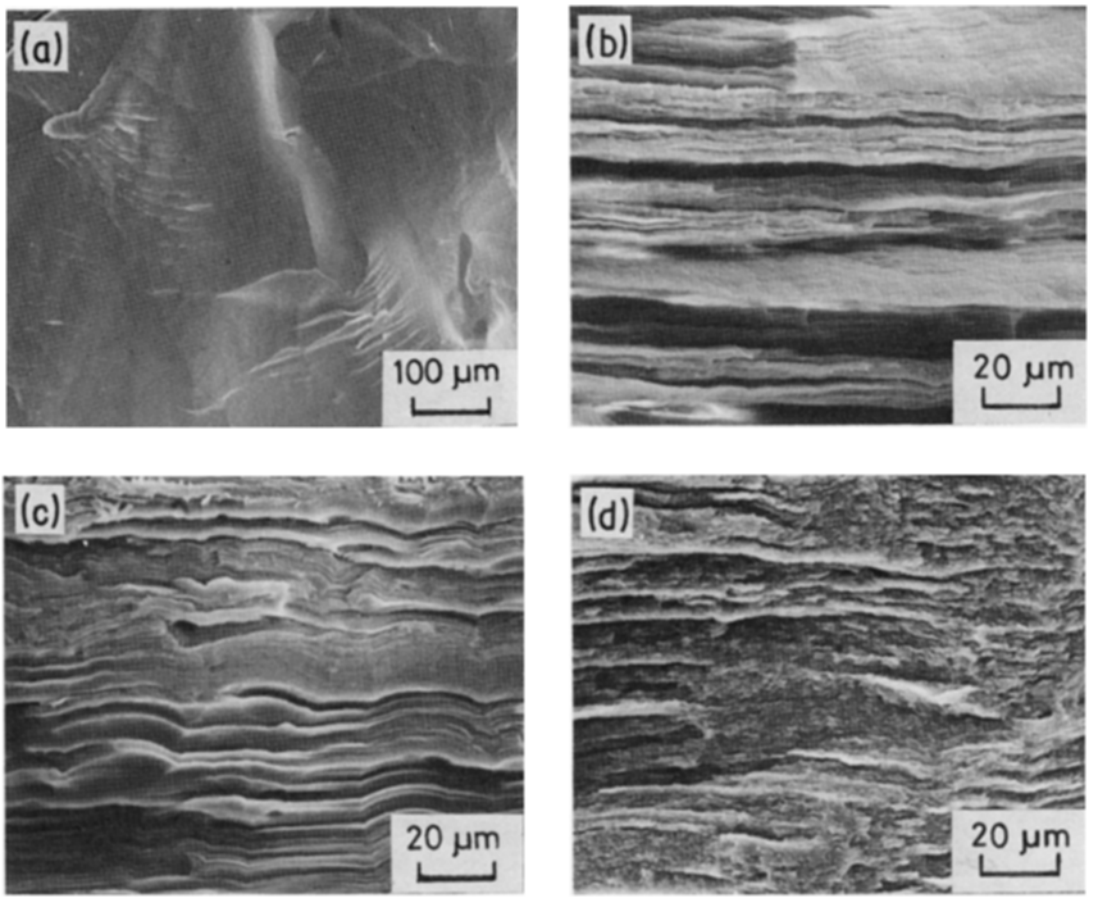

Figure 11 SEM-photographs of the fracture surface of the CVD-BN plates. (a) The t-BN plate prepared at a T_{dep} = 1400° C, P_{tot} = 30 torr in the A-region; (b) the t-BN plate prepared at a T_{dep} = 1800° C, P_{tot} = 30 torr in the B-region; (c) the (t + t′)-BN plate prepared at a T_{dep} = 1400° C, P_{tot} = 5 torr in the C-region; (d) the (t + h)-BN plate prepared at a T_{dep} = 1800° C, P_{tot} = 5 torr in the D-region.

Tagawa and Ishii [35] also investigated the effects of heat treatment on $c_0/2$ and Lc of powder prepared by the BCl_3–NH_3 reaction, and observed a similar temperature dependence. The above results indicate that the formation of a t-BN plate at a P_{tot} above 10 torr proceeds as follows: cluster (aggregate of polymers) formation in vapour phase → adsorption of cluster on the solid surface → decomposition of cluster due to heating.

At a P_{tot} of 5 torr, a CVD-BN plate formed at a T_{dep} of 1300 to 1600° C was a mixture of two kinds of t-BN different in $c_0/2$, whereas that formed at a T_{dep} of 1700 to 2000° C was a mixture of t-BN and h-BN. Takahashi *et al.* [20–22] obtained a mixture of t-BN and h-BN on iron and nickel substrates at a T_{dep} of 1000 to 1200° C. However, from the fact that their T_{dep} was very low and because the t′–BN obtained at a T_{dep} of 1300 to 1400° C in the present experiment had a $c_0/2$ close to that of h-BN but had no ($h\,k\,l$) reflections, their h-BN may be t′–BN.

A slight shoulder was observed at 2θ = 45.5° in the (1 0) band of (t + t′)-BN obtained at a T_{dep} of 1500 to 1600° C (Fig. 4c), which did not correspond to the (1 0 0), (1 0 1) or (1 0 2) reflections of h-BN. The shoulder not only appeared in the powdered samples but was also observed in the plate samples. Herold

TABLE I Literature data on the crystal structure of CVD-BN

Reference	Reactants/carrier	T_{dep} (° C)	P_{tot} (torr)	Structure	
				$c_0/2$(nm)	Lc(nm)
Adams and Capio [14]	B_2H_6 + NH_3/N_2	250–600	0.3–0.5	(Amorphous)	2.5
Miyamoto *et al.* [15]	B_2H_6 + NH_3/H_2	300	0.4	(Amorphous)	
Murarka *et al.* [13]	B_2H_6 + NH_3/Ar + H_2	300–900	760	(Amorphous)	
Rand and Roberts [8]	B_2H_6 + NH_3/H_2	600–900	760	((0 0 2)broad)	1.0–6.5
Hyder and Yep [11]	B_2H_6 + NH_3/H_2	700–1000	0.3–1	(Better crystalline)	
Hirayama and Shono [10]	B_2H_6 + NH_3/H_2	700–1250	760	0.334	
Motojima *et al.* [24]	BCl_3 + NH_3/Ar + H_2	250–700	760	(Amorphous)	
Takahashi *et al.* [20–22]	BCl_3 + NH_3/Ar + H_2	800–1200	760	0.333, 0.35	> 100.0, 2.0
Koide *et al.* [18]	BCl_3 + NH_3/N_2	900–1050	760	0.35–0.37	1.6–3.3
Malé and Salanoubat [5]	BCl_3 + NH_3	1450–1800	0.1–10	(Hexagonal form)	
Clerc and Gerlach [4]	BCl_3 + NH_3/H_2	1550–1850	0.8–2.2	(Anisotropic)	
Basche and Shiff [3]	BCl_3 + NH_3/?	1900	1	0.336–0.343	5.0–10.0
This work	BCl_3 + NH_3/H_2	1200–2000	5–60	0.333–0.36	1.0–> 100.0

et al. [42] reported r-BN (rhombohedral BN) with a lattice constant $a = 0.2504$ nm and $c = 1.001$ nm (in hexagonal indices) by melting B_2O_3 or $Na_2B_4O_7$ with KCN. Ishii *et al.* [43] heated the h-BN powder including oxygen in a graphite crucible in a N_2 atmosphere in a temperature range from 1750 to 2100° C, and showed the formation of filamentary crystals of r-BN ($a = 0.252$ nm, $c = 1.002$ nm) on the furnace wall at about 1500° C. r-BN yielded peaks at 2θ of 42.6° and 45.5° in the (1 0) band of t-BN. As seen in Fig. 4c, the peak of r-BN overlaps with that of the (1 0) band of t-BN at 2θ of 42.6°, while the peak position of 2θ of 45.5° is in good agreement with that of the shoulder ($2\theta = 45.5°$). Thus, it may be said that r-BN is included in (t + t')-BN. The structure of the commercially available CVD-BN (Union Carbide Corp.) is the same as that of the mixture of t-BN and h-BN obtained in the D-region.

t-BN obtained by the CVD method does not crystallize to h-BN by heat treatment up to 2200° C [44]. Crystallization occurs only at temperatures of at least 2300° C, under high pressures [44]. As shown in Fig. 6, the t'-BN formed at a P_{tot} of 5 torr and a T_{dep} below 1600° C, yielding the $(0\,0\,l)_H$ reflections, had a smaller $c_0/2$ than that of the t-BN formed at a P_{tot} above 10 torr and a T_{dep} of 2000° C. It is concluded that the variation in the crystal structures of the CVD-BN plates are not related to heat treatment after deposition. The crystal structure (t, t', h) of the CVD-BN plates markedly depends on the CVD conditions such as P_{tot} and T_{dep} as described above. At a P_{tot} of 10 torr and a T_{dep} of 1800° C, t-BN alone was formed as shown in Fig. 6, whereas h-BN was co-deposited by changing the gas-flow rate. Moreover, the change in gas-flow profile enabled preferential deposition of h-BN at the conditions for co-deposition of t-BN and h-BN. Fig. 12 is the X-ray diffraction pattern of the CVD-BN plate mainly consisting of h-BN, which was synthesized by changing the gas-flow profile at a T_{dep} of 2000° C and a P_{tot} of 5 torr. Fig. 13 is an SEM photograph of this CVD-BN plate (Fig. 12). It exhibits well-crystallized surface morphology, with each grain characterized by five-fold symmetry. The above results suggest that the variations in crystal structure of CVD-BN (t, t', h) depend markedly on the formation processes.

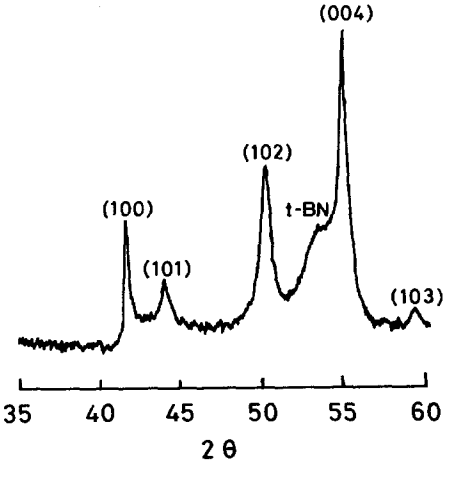

Figure 12 X-ray diffraction pattern of the CVD-BN plate consisting predominantly of h-BN.

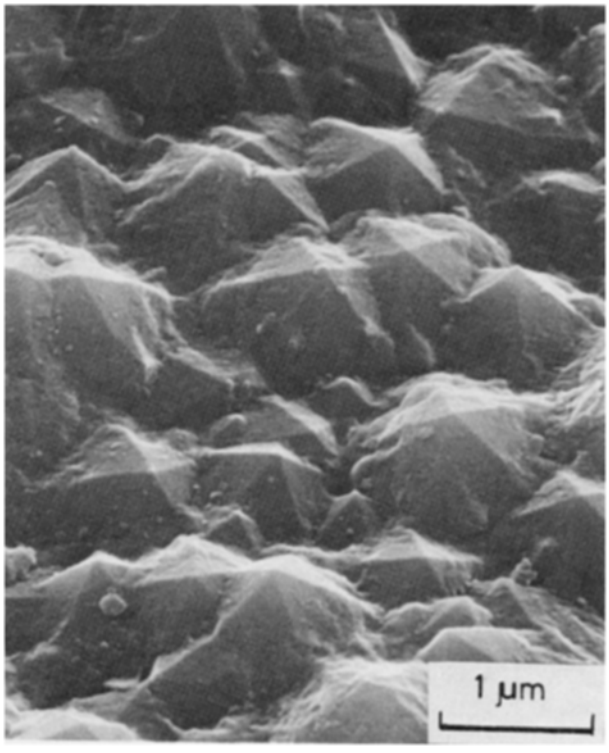

Figure 13 SEM-photograph of the deposition surface of the CVD-BN plate consisting predominantly of h-BN.

4.3. Microstructure of CVD-BN plate

Motojima *et al.* [24], Gafri *et al.* [19] and Takahashi *et al.* [20] indicated that the surface structure of CVD-BN was pebble-like. CVD-carbon, which has similar crystal structure to CVD-BN, also shows the pebble-like structure [45]. However, no researchers have reported the surface structure of CVD-BN or CVD-carbon which is composed of crystal facets. If a CVD-BN plate is a crystalline deposit and is composed of large crystallites, crystal facets should be observed on the surface. In this work, the surface structure composed of pyramidal pentagonal facets was observed on the CVD-BN plate consisting predominantly of h-BN as shown in Fig. 13, although the pebble structure (similar to Fig. 9b) was observed at low magnification. On the other hand, facets were not found in every t-BN plate even at high magnification.

A pebble in a t-BN plate is composed of fine grains under 0.1 μm in diameter independent of T_{dep}. A carbon black cluster, prepared by pyrolysis of hydrocarbon gas, is a spherical particle of several tens of nanometers in diameter [40]. Therefore, the fine grain shown in Figs. 10a and b may reflect the "cluster" mentioned in section 4.4. This implies that t-BN is formed by deposition of clusters grown in a vapour phase. In contrast to a t-BN plate, the surface structure of a (t + h)-BN plate is composed of larger grains, as the result of the co-existence of h-BN. The deposition surface of an h-BN plate shows the facet structure. This indicates that the deposition of h-BN occurs without first forming clusters.

Shiff [46] reported that the fracture surface of anisotropic CVD-BN showed a laminar structure. In this work, similarly, a laminar structure was clearly observed in the CVD-BN plates formed in the B-, C-

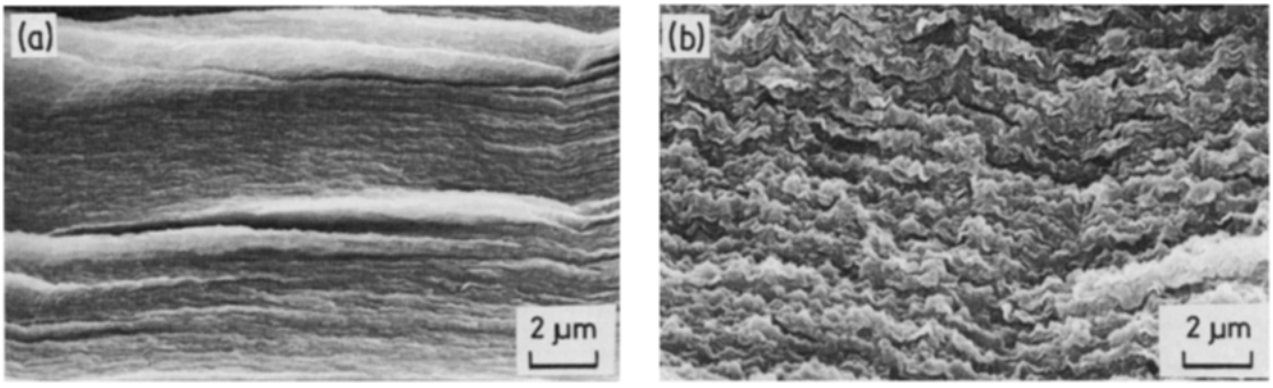

Figure 14 SEM-photographs of the fracture surface at a high magnification. (a) The (t + t′)-BN plate prepared at a T_{dep} = 1400° C, P_{tot} = 5 torr in the C-region; (b) the (t + h)-BN plate prepared at a T_{dep} = 1800° C, P_{tot} = 5 torr in the D-region.

and D-regions in Fig. 3 (Figs. 11b to d). However, the fracture surface of t-BN obtained in the A-region showed a glass-like fracture behaviour. This implies that t-BN is rather isotropic (Fig. 11a). This result closely corresponds to the result of the X-ray diffraction analysis (Fig. 8). Fig. 8 reveals that at a P_{tot} above 10 torr, a higher T_{dep} gave stronger orientation in the CVD-BN plates. This is consistent with the case observed on the CVD-carbon [47]. At a P_{tot} of 5 torr, however, low-T_{dep} deposits of (t + t′)-BN exhibited stronger orientation than high-T_{dep} deposits of (t + h)-BN. This phenomenon cannot yet be explained satisfactorily, but the difference in orientation between the (t + t′)-BN plates and the (t + h)-BN plates indicated in Fig. 8 appears also in the microstructure of their fracture surfaces. Fig. 14 is an SEM photograph at high magnification (× 5 000), which confirms the difference between the (t + t′)-BN plates and the (t + h)-BN plates, though both showed laminar structures in Fig. 11. The (t + t′)-BN plate in Fig. 14a shows a well-composed laminar structure, whereas the (t + h)-BN plate in Fig. 14b shows finely rippled layers. The degree of orientation of the (t + h)-BN plate shown in Fig. 8 is explained as a result of the microscopically-random orientation of the crystallites, although it has a macroscopically-laminar structure.

5. Conclusions

A CVD-BN plate was synthesized by the cold wall CVD method using the BCl_3–NH_3–H_2 gas system, and the effects of T_{dep} and P_{tot} on the structures were investigated. The conclusions are as follows:

1. 0.2 to 1 mm-thick CVD-BN plates were obtained. Transparent, semi-transparent, and opaque-white plates formed depending on the deposition conditions.

2. The crystal structure of the deposits was affected by P_{tot} and T_{dep}. t-BN was obtained at a P_{tot} of 10 to 60 torr and a T_{dep} of 1200 to 2000° C, and $c_0/2$ was smaller for higher T_{dep}.

3. At a P_{tot} of 5 torr, a crystallographic mixture of two different kinds of BN was formed. t-BN and h-BN co-deposited at a T_{dep} above 1700° C, whereas a mixture of two kinds of t-BN different in $c_0/2$ [(t + t′)-BN plate] deposited at a T_{dep} below 1600° C. The structurally different BN was considered to form due to different deposition processes.

4. It was suggested that r-BN was included in a (t + t′)-BN plate formed at a P_{tot} of 5 torr and a T_{dep} of 1500 to 1600° C.

5. h-BN and t-BN co-deposited at a P_{tot} of 5 torr and a T_{dep} above 1700° C; however, a preferential deposition of h-BN was also possible. The surface structure of the h-BN plate was characterized by five-fold symmetry.

6. At both conditions: P_{tot} = 5 torr, T_{dep} = 1300 to 2000° C; and P_{tot} = 10 to 60 torr, $T_{dep} \geqq$ 1600° C, an anisotropic CVD-BN plate with a *c*-plane oriented parallel to the deposition surface was obtained, whereas an isotropic CVD-BN plate deposited at a P_{tot} of 20 to 60 torr and a T_{dep} below 1400° C. Strongly oriented CVD-BN plates showed laminar structures, whereas an isotropic CVD-BN plate exhibited a glass-like fracture surface.

7. The as-deposited surface of the CVD-BN plates showed a pebble-like structure. The pebble was composed of fine grains of several tens to several hundred nanometers in diameter.

Acknowledgements

The study was performed under the Masumoto Amorphous and Intercalation Compounds Project, promoted by the Science and Technology Agency and the Research Development Corporation of Japan. The authors wish to thank the Project Director, Professor T. Masumoto of the Research Institute for Iron, Steel and Other Metals, Tohoku University, for his support and encouragement.

References

1. T. A. INGLES and P. POPPER, "Special Ceramics" edited by P. Popper (Academic Press, London, 1960) p. 144.
2. M. ISHII, *Bull. Ceram. Soc. Jpn.* **5** (1970) 467.
3. M. BASCHE and D. SHIFF, *Mater. Design Eng.* (*Feb*). (1964) 78.
4. G. CLERC and P. GERLACH, in Proceedings of the 5th International Conference on Chemical Vapour Deposition, Slough, England, September 1975, edited by J. M. Blocher Jr, H. E. Hintermann and L. H. Hall, (The Electrochemical Society, Inc. Princeton, 1975) p. 777.
5. G. MALÉ and D. SALANOUBAT, in Proceedings of the 7th International Conference on Chemical Vapour Deposition, Los Angeles, USA, October 1979, edited by T. O. Sedgwick and H. Lydtin (The Electrochemical Society, Inc, Princeton, 1979) p. 391.
6. J. THOMAS Jr, M. E. WESTON and T. E. O'CONNOR, *J. Amer. Chem. Soc.* **82** (1962) 4619.

7. R. S. PEASE, *Acta Cryst.* **5** (1952) 356.
8. M. J. RAND and J. F. ROBERTS, *J. Electrochem. Soc.* **115** (1968) 423.
9. W. BARONIAN, *Mater. Res. Bull.* 7 (1972) 119.
10. M. HIRAYAMA and K. SHONO, *J. Electrochem. Soc.* **122** (1975) 1671.
11. S. B. HYDER and T. O. YEP, *ibid.* **123** (1976) 1721.
12. T. KIMURA, K. YAMAMOTO and S. YUGO, *Jpn. J. Appl. Phys.* **17** (1978) 1871.
13. S. P. MURARKA, C. C. CHANG, D. N. K. WANG and T. E. SMITH, *J. Electrochem. Soc.* **126** (1979) 1951.
14. A. C. ADAMS and C. D. CAPIO, *ibid.* **127** (1980) 399.
15. H. MIYAMOTO, M. HIROSE and Y. OSAKA, *Jpn. J. Appl. Phys.* **22** (1983) L216.
16. D. BELFORTI, S. BLUM and B. BOVARNICK, *Nature* **4779** (1961) 901.
17. M. BASCHE, US Patent 3 152 006 (1964).
18. S. KOIDE, K. NAKAMURA and K. YOSHIMURA, *Nihon Daigaku Bunrigakubu Shizen Kagaku Kenkyusho Kenkyu Kiyo* **13** (1978) 13.
19. O. GAFRI, A. GRILL and D. ITZHAK, *Thin Solid Films* **72** (1980) 523.
20. T. TAKAHASHI, H. ITOH and A. TAKEUCHI, *J. Cryst. Growth* **47** (1979) 245.
21. T. TAKAHASHI, H. ITOH and M. KURODA, *ibid.* **53** (1981) 418.
22. T. TAKAHASHI, H. ITOH and A. OHTAKE, *Yogyo-Kyokai-Shi* **89** (1981) 63.
23. M. SANO and M. AOKI, *Thin Solid Films* **83** (1981) 247.
24. S. MOTOJIMA, Y. TAMURA and K. SUGIYAMA, *ibid.* **88** (1982) 269.
25. H. O. PIERSON, *J. Composite Mater.* **9** (1975) 228.
26. H. HANNACHE and R. NASLAIN, in Proceedings of the European Conference on CVD, Eindhoven, Holland, May 1983, edited by J. Bloem, G. Verspui and L. R. Wolff (Philips Centre for Manufacturing Technology, Eindhoven, The Netherlands, 1983) p. 305.
27. H. HANNACHE, R. NASLAIN and C. BERNARD, *J. Less-Common Metals* **95** (1983) 221.
28. H. HANNACHE, J. M. QUENISSET, R. NASLAIN and L. HERAND, *J. Mater. Sci.* **19** (1984) 202.
29. A. C. ADAMS, *J. Electrochem. Soc.* **128** (1981) 1378.
30. J. J. GEBHARDT, in Proceedings of the 4th International Conference on Chemical Vapour Deposition, Boston, Massachusetts, USA, October 1973, edited by G. F. Wakefield and J. M. Blocher Jr (The Electrochemical Society, Inc. Princeton, 1973) p. 460.
31. K. NAKAMURA, I. TOHYAMA and K. YOSHIMURA, in Synopses of the 1981 Spring Meeting of the Chemical Society of Japan, Tokyo, Japan (The Chemical Society of Japan, Tokyo, 1981) p. 280.
32. K. NAKAMURA, S. MISAWA and K. YOSHIMURA, in Synopses of the 1982 Spring Meeting of the Chemical Society of Japan, Tokyo, Japan (The Chemical Society of Japan, Tokyo, 1982) p. 452.
33. JANAF Thermochemical Tables, 2nd Edn., NSRDS-NBS 37, National Bureau of Standards (1971).
34. F. MEYER and R. ZAPPNER, *Berichte der Deutschen Chemischen Gesellschafft* **54** (1921) 560.
35. H. TAGAWA and K. ISHII, *Kogyo-Kagaku-Zasshi* **70** (1967) 617.
36. K. NIIHARA and T. HIRAI, *J. Mater. Sci.* **11** (1976) 593.
37. M. SOKOLOWSKI, *J. Cryst. Growth* **46** (1979) 136.
38. S. SHANFIELD and R. WOLFSON, *J. Vac. Sci. Technol.* **A1** (1983) 323.
39. M. SATOU and F. FUJIMOTO, *Jpn. J. Appl. Phys.* **22** (1983) L171.
40. J. BISCOE and B. E. WARREN, *J. Appl. Phys.* **13** (1942) 364.
41. S. NAKAMURA and Z. ARAI, *Nagoya-Kogyo-Shikenjo Report* **15** (1966) 205.
42. A. HEROLD, B. MARZLUF and P. PERIO, *Compt. Rend.* **246** (1958) 1866.
43. T. ISHII, T. SATO, Y. SEKIKAWA and M. IWATA, *J. Cryst. Growth* **52** (1981) 285.
44. A. W. MOORE, *Nature* **221** (1969) 1131.
45. S. YAJIMA and T. HIRAI, *J. Mater. Sci.* **4** (1969) 416.
46. D. SHIFF, *Met. Eng. Quarterly* **2**(4) (1962) 32.
47. T. HIRAI, *Trans. Jpn. Inst. Met.* **8** (1967) 190.

Received 22 March
and accepted 2 April 1985